YELLOW MN-RICH TOURMALINE FROM THE CANARY MINING AREA, ZAMBIA

Brendan M. Laurs, William B. (Skip) Simmons, George R. Rossman, Eric A. Fritz,
John I. Koivula, Björn Anckar, and Alexander U. Falster

The most important source of yellow gem elbaite is the Canary mining area in the Lundazi District of eastern Zambia. The tourmaline has been mined since 1983 from both pegmatite and eluvial/alluvial deposits, in colors typically ranging from yellow-green to yellow to orange and brown; much of the orange-to-brown material is heated to attain a "golden" or "canary" yellow color. The tourmaline is Mn-rich (up to 9.18 wt.% MnO documented in the literature) and contains traces of Ti and little or no Fe. The distinctive composition of this tourmaline is probably the result of the crystallization of abundant schorl from an unusual B-rich, Li-poor pegmatite magma, which depleted Fe while conserving Mn until the late-stage crystallization of gem pockets.

Since the early 1980s, gem-quality yellow elbaite has been intermittently mined from a small area in eastern Zambia. Marketed as Canary tourmaline since 2001, this material is notable for its vivid yellow color and high Mn content—among the highest ever recorded in any tourmaline (e.g., Shigley et al., 1986). Starting in 2002, organized purchasing and mining initiatives brought greater quantities of this elusive tourmaline to the market, particularly in Japan, where it has gained popularity and commanded high prices (Federman, 2002; "Supplier to vertically integrate…," 2004). Although most of the cut tourmaline available is in melee sizes (<0.20 ct), exceptional faceted stones up to 50 ct have been cut (figure 1).

Due to its unusual color and composition, this tourmaline attracted considerable attention in the mineralogical literature when it first entered the marketplace (see Nuber and Schmetzer, 1984; Schmetzer and Bank, 1984a; Rossman and Mattson, 1986; Shigley et al., 1986). While some of these articles did not specify the locality within Zambia, others stated "near Chipada," which refers to the largest town (Chipata) in eastern Zambia, located near the border with Malawi. However, there are no gem-bearing pegmatites in the Chipata area, and the actual locality is the Lundazi District, located ~160 km to the north (as indicated by Rossman and Mattson, 1986). Since the location was kept secret for many years, some more recent reports have named the source locality as Mozambique (Wong, 2001) or Malawi (e.g., Boehm, 2001; Federman, 2002). The enriched manganese content of this Zambian elbaite has led some authors to refer to it as *tsilaisite* (Schmetzer and Bank, 1983, 1984b; Kane, 1986).[a]

While in Zambia in August 2004, three of the authors (BML, WBS, and BA) visited the most important deposit for yellow elbaite, known as the Canary mining area, to gather information on the geology and production of this unusual material, and to obtain samples for gemological characterization and chemical analysis. Two days were spent at

---

See end of article for About the Authors and Acknowledgments.
GEMS & GEMOLOGY, Vol. 43, No. 4, pp. 314–331.

Figure 1. Commercial quantities of Mn-rich "canary" yellow elbaite come from just one deposit, the Canary mining area in eastern Zambia. Although the material is typically cut in melee sizes, this exceptional stone weighs 50.26 ct. Courtesy of Shire Trading Ltd.; photo © Harold & Erica Van Pelt.

the deposit with Tommy Wu (Shire Trading Ltd., Hong Kong), who was leasing the mine in partnership with a Zambian company. Since then, Mr. Wu has updated information on the mining and production, and supplied additional samples for our research.

LOCATION AND ACCESS

The Canary mining area is located at coordinates 12°23.764′ S, 32°53.471′ E, and ~1,440 m elevation. This position lies 32 km west-southwest of Lundazi (figure 2 inset), from which the deposit can be reached in about one hour by car on moderately well-maintained dirt roads. Two small villages are located near the mining area: Muchapansala and Chanyalubwe. The mining camp (figure 3) is powered by a generator and obtains drinking water from a well. The deposit can be worked roughly 10 months of the year, excluding the rainy season from late December to early February. In the past, the deposit also has been referred to as the Kaombeka or Doost-Chiwele mine (Njamu, 2003).

HISTORY AND PRODUCTION

Initial gem discoveries in the Lundazi District probably occurred in the late 1970s through activities of local villagers (Patney and Tether, 1988). The Canary mining area was originally worked for electronic-grade quartz (ca. 1982), and the brown tourmaline was tossed into the mine dumps (Njamu, 2003). Yellow tourmaline from eastern Zambia was first documented by Schmetzer and Bank (1983). It is likely that the material came from the Canary mining area (known as Kaombeka at the time), which is the most important source of this tourmaline in the area. A survey of the literature revealed only one other yellow tourmaline–producing site in the Lundazi District, which was mapped by O'Connor (1998) as the Chamunjili mine, located 18 km northeast of the Canary mining area. To the authors' knowledge, this locality has not been active for several years.

The first organized search for tourmaline in the Canary mining area occurred in 1987 (when it was still known as Kaombeka). At that time, the main pegmatite was worked by the Small Mines Unit of Zambian Consolidated Copper Mines (ZCCM). Although Zgambo (1995) reported that ZCCM removed 540 m^3 of material from two pits, yielding 242 kg of gem rough, the total production of tour-

---

[a] *Tsilaisite* is the name proposed by Kunitz (1929) for a hypothetical Mn-rich tourmaline end member, after the first locality where high-Mn tourmaline was documented (Tsilaisina, Madagascar). The term appeared in a list of new mineral names published by Dunn et al. (1985), although it had not been approved by the Commission on New Minerals and Mineral Names of the International Mineralogical Association. Tsilaisite was recently included in a list of discredited minerals (Burke, 2006), because no samples have been documented with sufficient Mn to attain the end-member composition. Therefore, we have placed the term in quotes when referring to the Mn-rich end-member composition in this article.

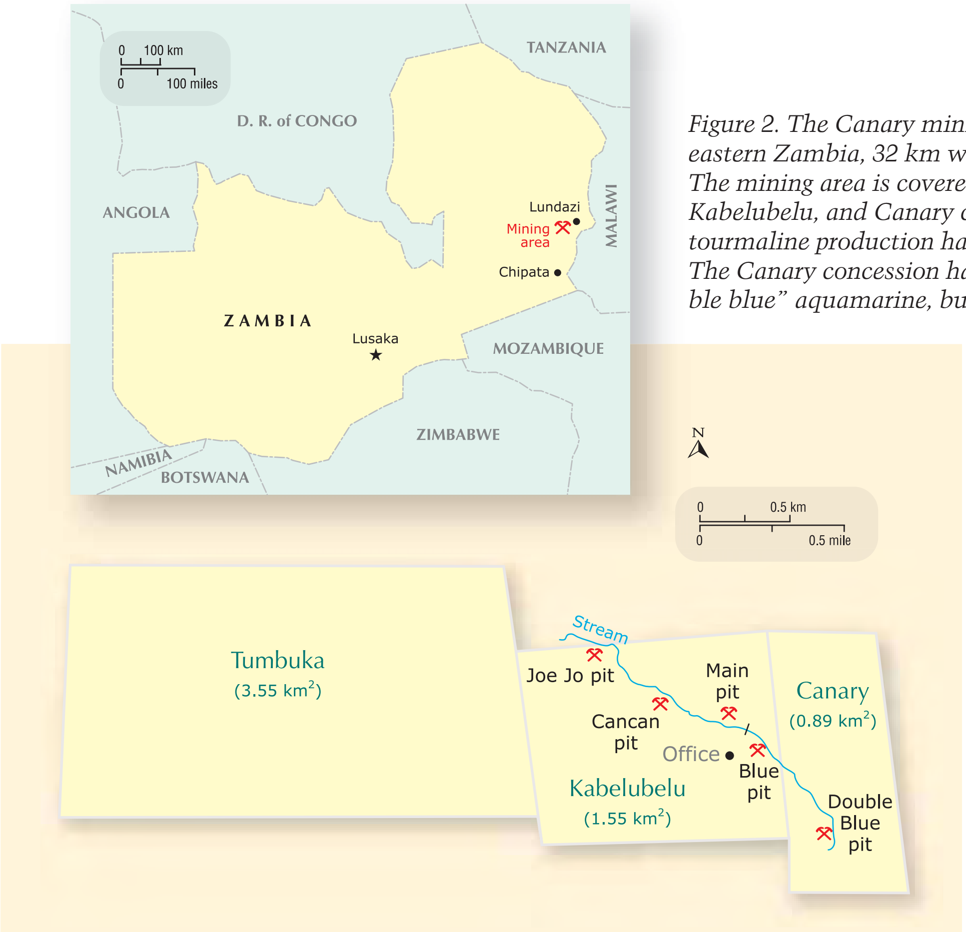

Figure 2. The Canary mining area is located in eastern Zambia, 32 km west-southwest of Lundazi. The mining area is covered by the Tumbuka, Kabelubelu, and Canary concessions. Most Canary tourmaline production has come from Kabelubelu. The Canary concession has been a source of "double blue" aquamarine, but not tourmaline.

maline (of all qualities) obtained by ZCCM was probably several tonnes (T. Wu, pers. comm., 2004). The largest single gem pocket was reportedly discovered in the mid-1990s by a subsequent owner; it produced approximately 3 tonnes of tourmaline, of which 0.5 tonne was of good gem quality (T. Wu, pers. comm., 2004). This pocket was found at a depth of about 4 m, and two smaller cavities—which yielded up to 100 kg of tourmaline—were encountered at approximately the same depth as mining proceeded to the east. As of November 1997, the deposit lay idle and the pit was filled with water (O'Connor, 1998).

In 2001, Mr. Wu together with Rita and Arun Mittal entered a purchasing agreement with as many as 60 local miners working the eluvial and alluvial deposits. They began creating a market for yellow tourmaline in Japan (and, to a lesser extent, in the U.S. and Europe) with gems cut from 3–4 kg of good-quality rough material. In late 2002, Mr. Wu and the Mittals formed a partnership to lease the area under the name Canary Mining Ltd. By the end of 2002, Canary Mining had amassed ~800 kg of rough tourmaline. Most of this would cut small stones of 3 mm or less, but a few large gems (e.g., 30, 14, and 11 ct) also were faceted.

In February 2003, Canary Mining began working secondary deposits near the original pegmatite, with modest results over the next five months. From December 2003 to August 2004, they used an excavator to explore primary deposits on the property (figure 4). However, they did not recover any tourmaline from the new areas tested, and the main pit appeared to be exhausted. Subsequent work has focused on intermittently mining the secondary deposits, typically producing 30–40 kg per month (or ~2 kg of tourmaline per day, consisting of 500–800 g of good gem rough). The 50 ct tourmaline in figure 1 was cut from this material (T. Wu, pers. comm., 2006).

In July 2007, Canary Mining Ltd. was acquired by Canary Gemstone International DMCC, a holding company formed in Dubai, with Mr. Wu and Mrs. Mittal as major shareholders. The influx of capital obtained through this venture will allow for the expansion of mining activities in 2008.

Figure 3. The mining camp for Canary tourmaline, shown here in the dry season (August), is located in a remote part of the Lundazi District. Photo by W. B. Simmons.

GEOLOGY

Pegmatites in the Lundazi area are known for producing mica and gem-quality aquamarine, spessartine, tourmaline (green, pink, or yellow), and rose quartz. These pegmatites and their gems have been described by Thomas (1982), Patney and Tether (1988), Zgambo (1995), Johnson et al. (1997), Milisenda et al. (2000), and Njamu (2003). Patney and Tether (1988) defined two belts of gem-bearing pegmatites in the Lundazi District, and indicated that they are broadly synchronous with the late Pan-African Sinda Batholith (~489 million years old [Ma]). Snelling et al. (1972) dated an undeformed pegmatite near Lundazi at 485 Ma.

The Canary mining area is underlain by Precambrian metamorphic rocks of the Irumide Foldbelt (e.g., Johns et al., 1989). O'Connor (1998) mapped the deposit within leucocratic gneiss (containing biotite, garnet, and sillimanite) of the Lumezi Gneiss Group. Deep soils cover the area, and the best exposures of the basement rocks are found in some mining pits and along the stream that crosses the mining claims.

The main pegmatite in the Canary mining area

Figure 4. Canary Mining Ltd. used a large excavator to explore primary deposits from December 2003 to August 2004. The main pegmatite is being mined down-dip from the area that produced large amounts of tourmaline in the mid-1990s; Asok Napa (in the foreground) was the mine's general manager during that time. Photo by Tommy Wu.

Figure 5. The contact between the footwall of the main pegmatite and the weathered host rock is marked by the sharp boundary to the right of the hammer (see yellow line). The hammer is sitting on the medium-grained border zone, which is separated from the coarse-grained feldspar-rich intermediate zone by a vein of black tourmaline + K-feldspar. Photo by B. M. Laurs.

is a lens-shaped body that discordantly intrudes biotite gneiss; it strikes east-west (~100°) and dips moderately south. At the time of the authors' 2004 visit, a large open pit (~16 m deep) partially filled with water marked the site where most of the pegmatite had been removed. Based on the extent of the workings, the pegmatite is believed to have been at least 60 m long and perhaps 18 m at its widest point (Njamu, 2003). Exposures of the footwall showed a medium-grained border zone (~15 cm wide) and in places a discontinuous aplitic zone that abruptly transitioned into a coarse-grained intermediate zone consisting mainly of K-feldspar and subordinate sodic plagioclase (figure 5). The hydrothermal leaching of quartz had resulted in vugs that contained euhedral overgrowths of albite and black tourmaline needles. We also observed conspicuous veins (up to 10 cm thick) of black tourmaline ± K-feldspar + albite cross-cutting the pegmatite. The host gneiss adjacent to the pegmatite was locally biotized and tourmalinized near the contact, but the minimal alteration overall indicated that the pegmatite had little interaction with the wallrock.

The large cavity found in the mid-1990s was in the central-northwestern part of the pit, in or near the core of the pegmatite. This pocket also contained abundant quartz crystals and "cleavelandite" feldspar. Although remains of these minerals were found on the mine dump, there was no evidence of any micas, such as the lepidolite that is commonly associated with gem tourmaline in granitic pegmatites.

The Canary deposit is distinctly different from other gem-bearing pegmatites in the area in that it lacks micas and is not a source of aquamarine. Zgambo (1995) indicated that rose quartz, mica, beryl, and gem-quality pink tourmaline were encountered during mining in 1987, but no evidence of these minerals was seen during our visit. There was also no evidence of the allanite, magnetite, and blue/pink/green tourmaline that were reported by Njamu (2003). One of the present authors (BA) noted some spessartine in the mine dumps in 2003, but no garnet was seen in the pegmatite itself.

A reconnaissance survey of past workings in the surrounding area during the authors' visit revealed two additional pegmatites with similar mineralogy, but they were much smaller than the main pegmatite and reportedly did not yield any gem tourmaline *in situ* (T. Wu, pers. comm., 2004). In addition, pegmatites with a distinctively different mineralogy were seen in the area. These quartz-rich pegmatites contained biotite (in sparse amounts, and typically no schorl) as the mafic mineral, and formed segregations in a granitoid rock or cross-cutting dikes in biotite gneiss. They were mined for dark blue (or "double blue") aquamarine (Laurs, 2004), which is frozen within the pegmatites rather than forming in cavities; therefore, the beryl rarely yields cut stones larger than 0.5 ct. Ductile deformation (the presence of bent and deformed crystals) of the beryl-bearing pegmatites indicated that they are older than the undeformed feldspar- and black tourmaline–rich type of pegmatite that contains Canary tourmaline. In places the deformed pegmatites underlie the eluvial deposits mined for tourmaline,

Figure 6. Secondary deposits downslope from the main Canary pegmatite are typically mined to a depth of 1–1.5 m (left). The miners recovered the gem rough by wet-screening the excavated material using water from a flooded mining pit (right). Photos by B. Anckar, June 2003.

which has created confusion about the original source of this gem material. O'Connor (1998) also documented at least two phases of pegmatites in this part of the Lundazi District, and indicated that the magnetic signature of the area suggests it may be underlain by a large granitic body.

According to Mr. Wu, other pegmatites located within a few kilometers of the Canary mining area have produced spessartine and chrysoberyl.

MINING AND PROCESSING

The Canary mining area consists of three mining concessions, covering a total of 600 ha (6 km^2). From west to east, these are the Tumbuka, Kabelubelu, and Canary licenses (again, see figure 2). During the authors' visit in 2004, 13 workings were seen, most of which were located on the Kabelubelu concession. These ranged from large open pits to small exploration trenches, in both primary and secondary (alluvial and eluvial) deposits.

Most of the Canary tourmaline produced since 2000 has come from the Kabelubelu concession, from secondary deposits located downslope of the main pegmatite. Mining was done by hand (figure 6, left) or with a small excavator to a depth of ~1–1.5 m (exceptionally, down to 5 m). The most favorable soil horizon for tourmaline was marked by a concentration of quartz fragments or pebbles. Miners wet-screened the material using 4 × 4 mm mesh (figure 6, right) or processed it through a simple washing plant (figure 7) consisting of a cement mixer, vibrating screens with mesh from 5 cm to 1 cm, and a sorting table (Njamu, 2003). Using water from a seasonal stream that flows through the mining area, the washing plant can process about 10–12 tonnes of material per day.

Mining of the primary deposits (for both tourmaline and aquamarine) was done using a large excavator (again, see figure 4), a pneumatic hammer, and by hand with picks, shovels, pry bars, hammers, and chisels. To avoid breaking the gem material, Canary

Figure 7. The washing plant that is also used to process material from the secondary deposits consists of a cement mixer followed by a series of vibrating screens. The water tank is filled from a small reservoir made in a seasonal stream that flows through the mining area. Photo by B. M. Laurs.

Figure 8. The yellow tourmaline in this slab (2.2 cm wide) is cut by veins and masses of black and brown tourmaline and brownish pink K-feldspar. A brecciated texture resulted from the late-stage influx of the tourmaline + K-feldspar. Photo by W. B. Simmons.

Mining Ltd. has limited the use of explosives. Since 2003, the mine has employed up to 20 workers from local villages, who are paid a salary and provided three meals a day (T. Wu, pers. comm., 2004).

The rough is sorted in Lusaka, and the material suitable for faceting (about 5–10% of the production) is cut in Bangkok. As mined, the tourmaline ranges from yellowish green to yellow, orange, and brown. Large pieces (up to 40 kg) have been recovered, but these typically consist of a brecciated assemblage of yellow to brownish yellow tourmaline that has been fractured and intruded by black/brown tourmaline ± K-feldspar (figure 8), requiring extensive processing to obtain small pieces of gem rough. However, some high-quality transparent yellow areas have been found within such material (figure 9). The veinlets of black tourmaline may show a scalloped texture along their planes of contact with the yellow tourmaline (figure 10), which suggests that the fractures were etched by hydrothermal fluids before being intruded by the schorl.

About 30% of the tourmaline is vivid yellow as mined. After being pre-formed, most of the other colors are heat treated to 500°C (and again to 550°C, as needed) in air to reduce the brown/orange component (see figure 19 of Kane, 1986). Heating does not always completely remove the brown hue (even after the second treatment), and it has no effect on the green component (T. Wu., pers. comm., 2006). The resulting hues range from bright yellow to brownish yellow to yellowish green (figures 11 and 12). Preliminary experiments at higher temperatures have succeeded in creating a pinkish red color from brownish yellow material (see box A).

According to Mr. Wu, most of the Canary tourmaline is faceted as calibrated stones in a variety of common shapes, in sizes ranging from 2 mm to 10 × 8 mm. About 5% of the production consists of larger stones that are faceted in free sizes, typically around 1 ct, with a very few stones in the 1–5 ct range. Briolettes have been cut from material containing minute fluid inclusions (figure 13). As of November 2007, enough rough material had been stockpiled to produce an estimated 20,000 carats of small (2–3 mm) cut stones.

Figure 9. These two views show a sample (6.5 cm in maximum dimension) containing a central core of gem-quality yellow tourmaline that is surrounded and partially cross-cut by black tourmaline (schorl). Courtesy of Shire Trading Ltd.; photos by Robert Weldon.

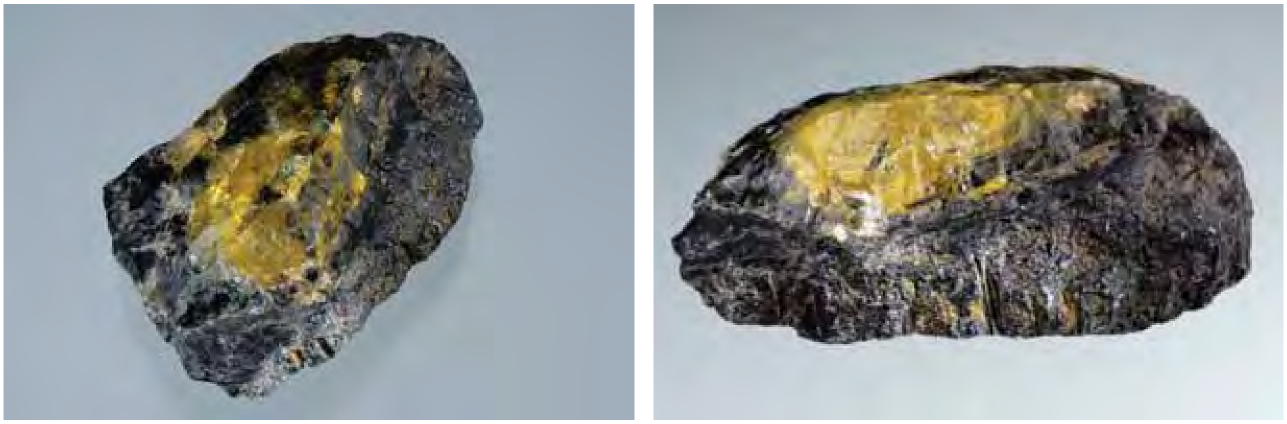

Figure 10. A distinctive scalloped pattern is visible at the interface between a cross-cutting veinlet of schorl and the surrounding tourmaline. Photomicrograph by J. I. Koivula; field of view is 2.5 mm.

Canary tourmaline publicly debuted in the gem trade at the International Jewellery Tokyo show in January 2001 ("Capturing the Canary...," 2003). Until the middle of this decade, most of the production was sold in Japan, but then demand shifted toward manufacturers in Thailand and Hong Kong that produce mass-market jewelry for U.S. customers ("Substantial increase in sales...," 2005).

In addition to the yellow elbaite, black tourmaline from the Canary mining area has been polished into beads and cabochons for the Japanese market. This schorl also has been powdered for use in the cosmetics industry in Japan.

MATERIALS AND METHODS

Thirty-one Canary tourmalines were gemologically characterized at GIA: five unheated cabochons (5.38–18.02 ct) and 26 heat-treated faceted stones (0.38–2.16 ct). We measured refractive indices with a Duplex II refractometer. Specific gravity was calculated by the hydrostatic method with a Mettler CM1200 electronic balance. Fluorescence to UV radiation was documented in a darkened room using a standard 4-watt long-wave (365 nm) and short-wave (254 nm) UV lamp. We also examined the samples with a Chelsea filter and a desk-model spectroscope. Internal features were observed using a standard binocular gemological microscope.

The chemical composition of 21 grain mounts of unheated yellow-to-orange-to-brown and yellow-green tourmaline (from one to six analyses per sample) was measured by electron microprobe at the

Figure 11. These unusually large (7.32–12.60 ct) heated Canary tourmalines show the yellow to "golden" yellow color range that is typical of this material. Courtesy of Shire Trading Ltd.; photo by C. D. Mengason.

Figure 12. These unheated cabochons (10.45–18.02 ct) and heated cut stones (1.92 and 2.16 ct; GIA Collection nos. 37339 and 37340) have a distinctive yellowish green color that is less common in Canary tourmaline than the yellow to "golden" yellow. All of these samples were gemologically characterized for this report. Courtesy/gift of Shire Trading Ltd.; photo by Robert Weldon.

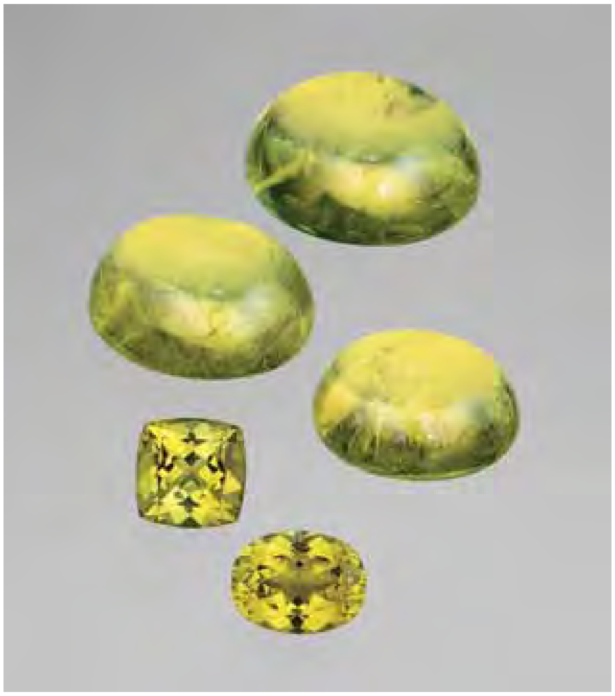

Box A: Preliminary Study of Higher-temperature Heat Treatment of Canary Tourmaline

Andreas Ertl (andreas.ertl@A1.net)
Institut für Mineralogie und Kristallographie, Universität Wien, Austria
George R. Rossman

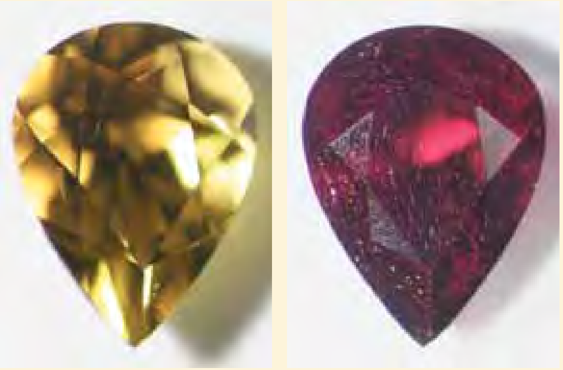

Figure A-1. This 0.18 ct Mn-rich tourmaline from the Canary mining area turned brownish yellow after conventional heating to 550°C (left) and brownish red after higher-temperature treatment to 700°C (right). Photos by A. Wagner.

Most Canary tourmaline is heat treated to 500–550°C to reduce the brown/orange component and produce the characteristic bright yellow coloration. Pieczka and Kraczka (2004) pointed out that heating of Mn^{2+}-bearing tourmalines above ~550°C initiates oxidation. Therefore, the yellow coloration would be expected to change to pink-red when Mn^{2+} is oxidized to Mn^{3+}. To investigate the effect of treating Canary tourmaline at higher temperatures, a faceted brownish yellow sample was heated to 700°C for 20 hours in air, using a Nabertherm furnace. The sample had been previously heated to 500–550°C to bring out the yellow color (figure A-1). This elbaite was Mn-rich (~6.5 wt.% MnO) and poor in Fe, Ti, Mg, Cr, and V, which were below the detection limits of X-ray energy-dispersive spectral (EDS) analysis. (However, the instrument used, a JEOL-EDAX analytic system, had relatively high detection limits for iron and titanium, at ~0.3 wt.% FeO and TiO_2.) A slow heating/cooling rate was employed (50°C/hour) to reduce the possibility of fracturing.

After heating, the brownish yellow sample was brownish red (figure A-1), as expected for the oxidation of Mn^{2+} to Mn^{3+} (the visible-NIR absorption spectrum [figure A-2] showed a broad band near 532 nm, which is due to Mn^{3+}). The brown component of the red color probably resulted from traces of Fe in the sample (below the detection limit of the EDS analysis), as indicated by weak Fe bands in the absorption spectrum. Therefore, the heat treatment of very-low iron material would be expected to yield a purer pink-red coloration.

In addition, two slabs of yellow-green tourmaline that were heated for seven days at 700°C or for five days at 750°C also showed distinct changes. These slabs turned nearly opaque, but were dark orangy red when viewed through very thin edges. Both of those samples experienced a total loss of hydroxide, as observed in their Raman spectra.

After heating, we observed pervasive tiny cracks in all samples, which most likely were caused by the release of water during the oxidation process. It is possible that such cracking could be minimized by heating the tourmaline to lower temperatures (>600°C but <700°C) and/or a shorter time, but additional experiments would be needed to test this.

Gamma-irradiation experiments on brownish yellow Zambian Mn-bearing elbaite by Reinitz and Rossman (1988) also generated a pink-red color. In their sample, they documented a decrease in the intensity of the Mn^{2+} absorption bands and a corresponding increase in the Mn^{3+} band. This irradiation mechanism does not remove hydroxide from the crystal and is a fundamentally different way of generating Mn^{3+} than the high-temperature oxidation.

Figure A-2. The visible-NIR absorption spectrum of the heated brownish red tourmaline in figure A-1 shows features related to Mn^{3+}, Fe^{2+}, and OH.

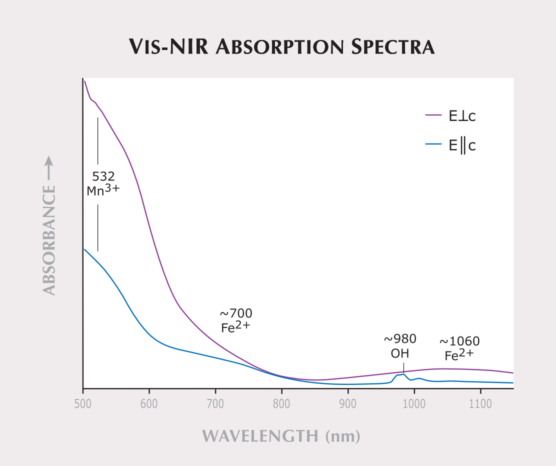

University of New Orleans. Also analyzed were eight of the faceted stones that were gemologically characterized for this study: four yellow to orangy yellow and four yellowish green. Data were collected using an ARL-SEMQ electron microprobe with 15 kV (for sodium) and 25 kV accelerating voltages, 15 nA beam current, and 3 µm beam diameter. The measurements were calibrated with natural mineral and synthetic compound standards, and a ZAF correction procedure was applied to the data.

To investigate the origin of color before and after heating, we first oriented a brownish orange sample using the optical interference pattern and then sliced and polished it so that the c-axis lay in the plane of the slices. We prepared one slice for spectra in the visible and near-infrared region (2.59 mm thick; 350–1100 nm) and another for spectroscopy in the UV–near Vis region (0.59 mm thick; 250–450 nm). We retained a portion of each slice in its unheated state and then heated the remaining portions (packed in sand) at a rate of 10°C/minute to 550°C, where they were held for two hours before they were cooled at 20°C/minute. We obtained spectra on transparent 340 × 340 µm areas of the heated and unheated samples using a custom-made microspectrometer with a silicon diode-array for the visible region, an indium-gallium-arsenide diode-array for the near-infrared region, and a silicon CCD detector for the UV–near Vis region.

We also prepared and treated a yellow-green sample using the same procedure as for the brownish orange sample, but it did not change color on heating to 600°C for two hours in air, so no further testing was done on it. One faceted brownish yellow Canary tourmaline that had previously been heated to 500–550°C was subjected to further heating to 700°C (again, see box A). In addition, two yellow-green slabs (0.9 and 1.7 mm thick) were heated in air to 500°C (two hours), 600°C (two hours), 700°C (seven days, one sample), and 750°C (five days, the other sample). Results for the latter two experiments are also described in box A (no changes in coloration were seen after the first two heating sessions).

RESULTS

Gemological Properties. The gemological properties of these Zambian samples are summarized (and compared to yellow tourmalines from Kenya; see Discussion) in table 1. Of the 31 Canary tourmalines, 11 were yellowish green (e.g., figure 12) and 20 were yellow to orangy yellow (figure 14). Microscopic

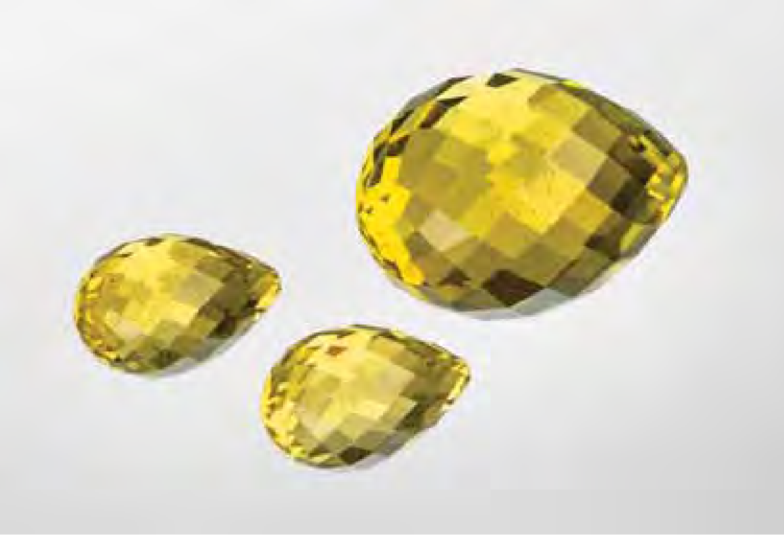

Figure 13. These briolettes of Canary tourmaline are notable for their large size. The largest stone is 65.74 ct, and the combined weight of the matched pair is 26.70 ct. Due to the presence of fluid inclusions, which can cause the material to fracture, none of the stones have been heated. Courtesy of Joeb Enterprises, Solana Beach, California; photo by C. D. Mengason.

Figure 14. Gemological properties were collected on these yellow to orangy yellow heated Canary tourmalines (0.38–1.79 ct). Gift of Shire Trading Ltd., GIA Collection nos. 37333–37338; photo by Robert Weldon.

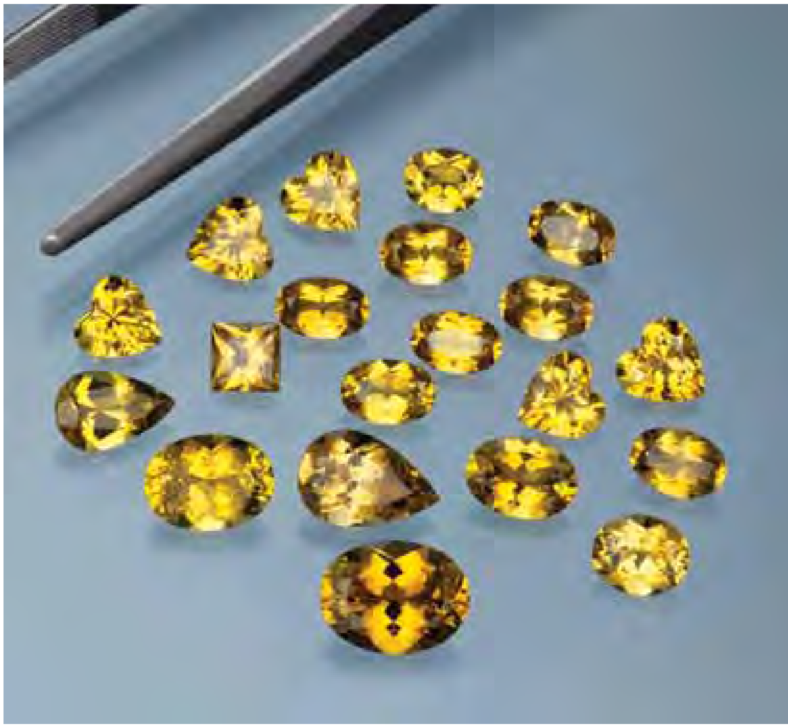

TABLE 1. Gemological properties of yellow tourmaline from Zambia and Kenya.

Properties	Zambia[a] Elbaite	Kenya[b] Dravite-uvite
Color range	Yellowish green or yellow to orangy yellow	Greenish yellow or yellow to brownish yellow
Pleochroism	Yellowish green, yellow, or orangy yellow to pale yellowish green, yellow, or orangy yellow	Yellow or orangy yellow to pale yellow or greenish yellow
RI (spot)	1.62	
n_o	1.645–1.649	1.642–1.650
n_e	1.623–1.625	1.619–1.630
Birefringence	0.020–0.025	0.020–0.023
SG	3.11–3.17	3.04–3.05
UV fluorescence		
Long-wave	Inert	Inert
Short-wave	Inert	Inert to moderate yellow
Chelsea filter	No reaction	No reaction
Absorption spectrum	General absorption to ~460 nm	Wide 440 nm band or general absorption to 480 nm
Internal features	Growth tubes, groups of two-phase (liquid-gas) fluid inclusions, and planar fluid inclusions	Small growth tubes, fluid inclusions, and two-phase (liquid-gas) inclusions

[a] *Data from this study. Slightly lower RI and SG values were reported for two samples by Boehm (2001): 1.620–1.641 and 3.10, respectively. Milisenda et al. (2000) give a lower SG value (3.05) for yellow tourmaline from Zambia.*

[b] *Data from Hänni et al. (1981), Johnson and Koivula (1996), and Simonet (2000).*

observation revealed internal features that are typical of tourmaline (figure 15), such as growth tubes, groups of two-phase (liquid and gas) inclusions along healed fractures, planar fluid inclusions, and a few angular primary three-phase fluid inclusions. The majority of the stones also contained transparent linear growth zoning. In general, the yellow to orangy yellow samples were small (<1.80 ct) and of high clarity; two were devoid of any internal features and showed only minor abrasions. The yellowish green stones ranged from slightly included (faceted stones) to moderately included (cabochons).

The physical properties of all samples were remarkably similar, regardless of color or heat treatment, except that the unheated stones contained more two-phase inclusions. This is consistent with the fact that (to reduce the risk of breakage) only very clean material is heat treated. There were no differences in the RI and SG values, or reaction to UV radiation, between the two color groups or the heated/unheated stones.

Chemical Composition. The electron-microprobe analyses showed that all samples were elbaite (e.g., figure 16), with 1.14–7.59 wt.% MnO and 0.04–0.54 wt.% TiO_2; iron was typically below the detection limit (0.016 wt.% FeO), but in rare cases it ranged up to 0.21 wt.% FeO (see table 2 and the *G&G* Data Depository). The faceted stones had compositions similar to those of the rough stones, except for a narrower range of Mn contents (~4–6.5 wt.% MnO) and no Fe was detected. The enriched Mn and low Fe content of Canary tourmaline is evident in figure 17.

UV-Vis-NIR Spectroscopy. Absorption spectra were collected on two sets of slices cut from a brownish orange sample that was heated to yellow (e.g., figure 18). The UV–near Vis spectra of both slices showed a

Figure 15. Inclusions seen in Canary tourmaline (particularly in unheated samples) include a group of secondary two-phase (liquid-gas) fluid inclusions that appear to have developed as the result of fracture healing (left, magnified 45×); growth tubes oriented parallel to the optic axis (or c-axis) direction (center, magnified 30×); and angular primary three-phase fluid inclusions (right, magnified 30×). Photomicrographs by J. I. Koivula.

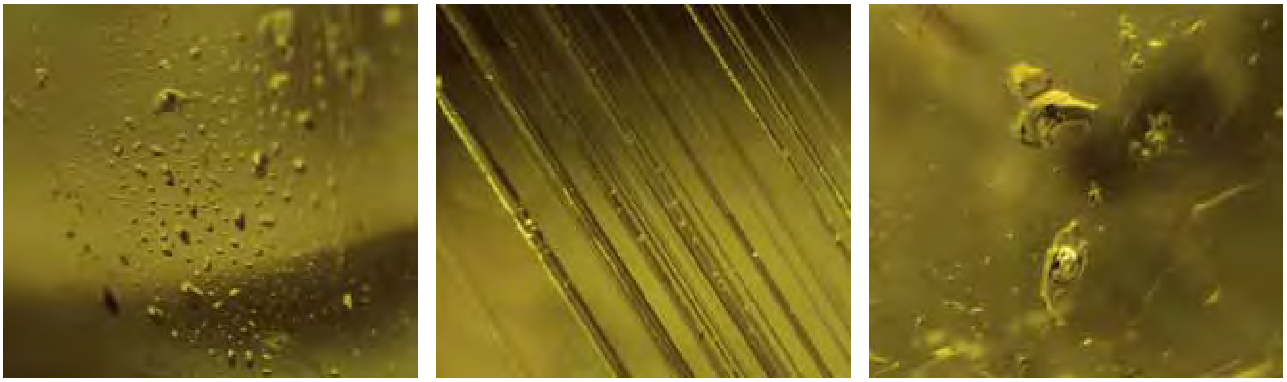

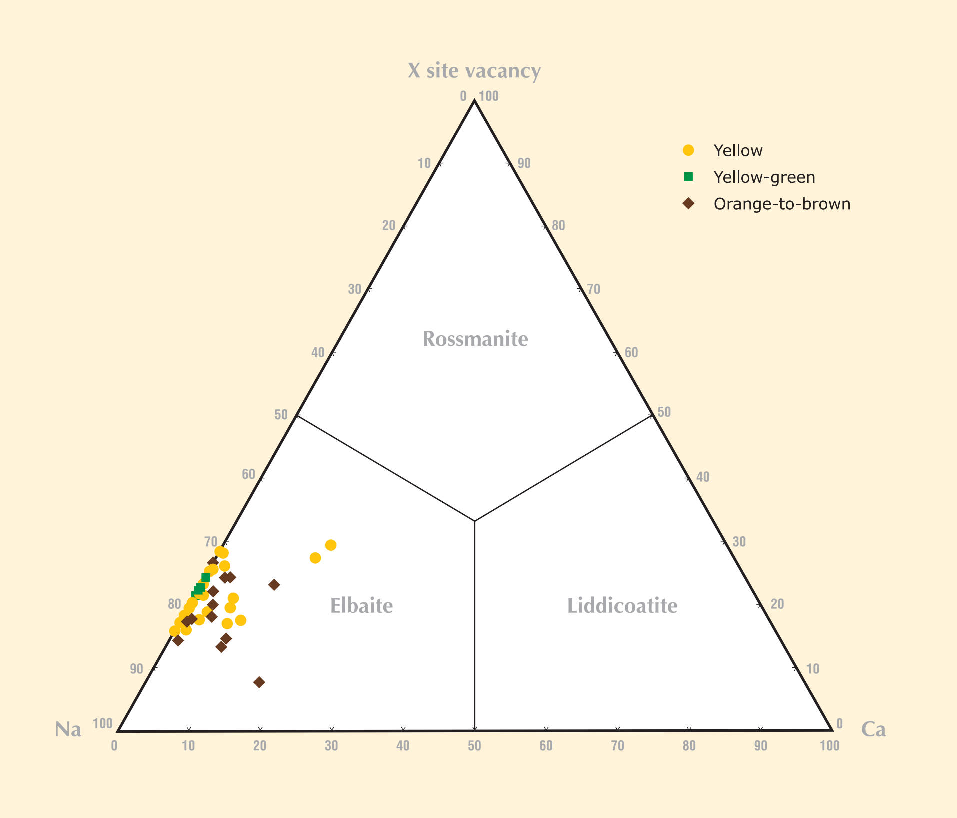

Figure 16. All the tourmaline samples analyzed by electron microprobe were elbaite. Shown here are the data for the rough samples; the compositions of the faceted stones overlapped the area occupied by these samples.

Figure 17. The Mn-rich, Fe-poor composition of Canary tourmaline is clearly illustrated by this plot, which shows the atoms per formula unit (apfu) of these elements. Also indicated for comparison is the Mn content required to attain the hypothetical Mn tourmaline end member "tsilaisite."

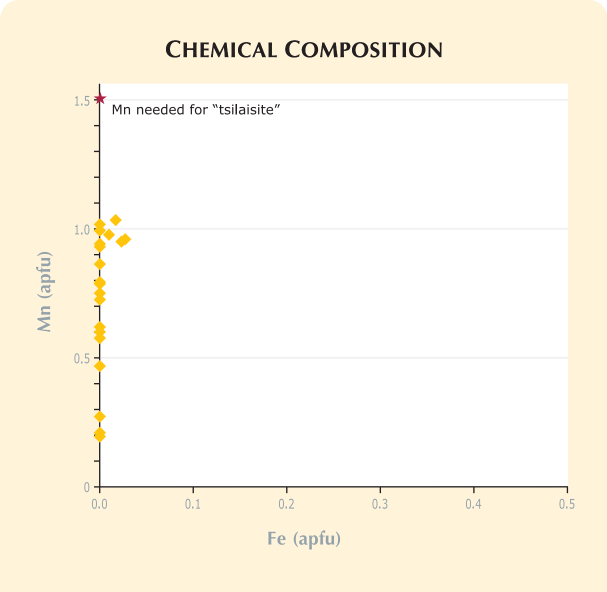

broad band at ~320 nm due to Mn^{2+}-Ti^{4+} intervalence charge transfer (IVCT), which was only slightly more pronounced in the heated sample (figure 19). The tail of this feature extended into the visible region, causing absorption of the violet-to-blue wavelengths (figure 20). The unheated sample showed both Mn^{2+}

Figure 18. These two slabs (~8 mm tall) were cut from the same piece of rough, and oriented with the c-axis in the plane of the slices. The brownish orange slab is unheated, while the yellow slice was heated for two hours at 550°C.

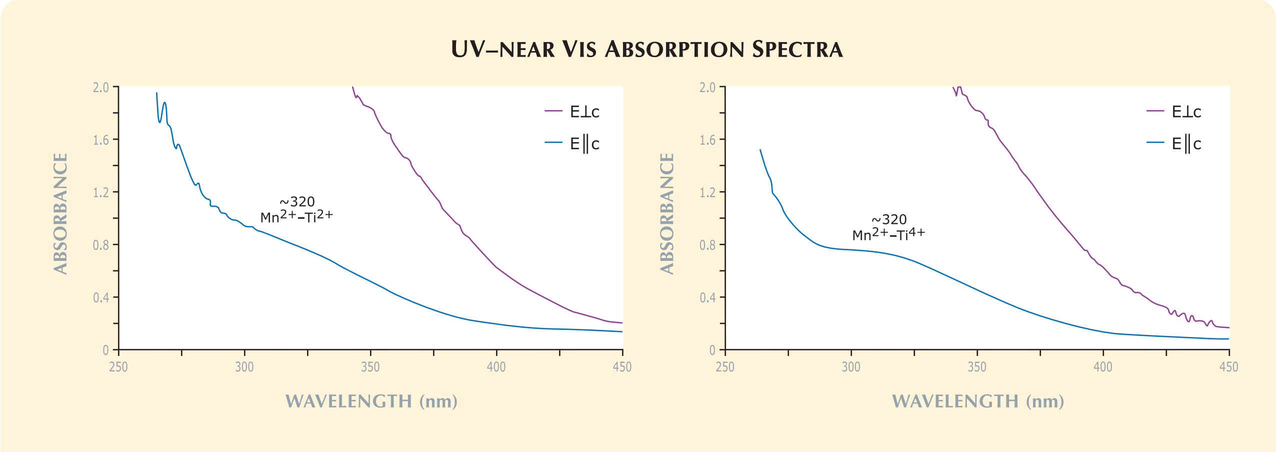

Figure 19. These UV–near Vis absorption spectra were collected on unheated brownish orange (left) and heat-treated yellow (to 550°C; right) slices of tourmaline (each 0.59 mm thick). No significant differences are seen after heating.

(sharp band at ~412 nm) and Mn^{3+} (band centered at 532 nm) features in the Vis-NIR spectra (Rossman and Mattson, 1986; Reinitz and Rossman, 1988). The Mn^{3+} band was absent from the heated sample, but that was the only change observed. Weak broad bands near 700 and 1060 nm are associated with Fe^{2+} (Mattson and Rossman, 1987). An Fe^{2+} band near 700 nm overlaps a Mn^{3+} band in the same region (Reinitz and Rossman, 1988). Features near 980 nm are overtones of the OH-stretching vibrations (Rossman and Mattson, 1986).

DISCUSSION

Gemological Properties. The gemological properties of the Canary tourmalines are typical for Mn-rich elbaite, and are comparable to those given in previous reports on yellow Zambian tourmaline (see Schmetzer and Bank, 1984b; Kane, 1986; Shigley et al., 1986; Milisenda et al., 2000; Boehm, 2001). Note, though, that none of our rough or cut samples exhibited the black needle-like inclusions mentioned in the literature (e.g., Boehm, 2001; Genis, 2001). According to Mr. Wu, such needles typically occur in the greenish yellow material but are usually removed during the cutting process.

For comparison, table 1 summarizes the properties of yellow tourmaline from Kenya, the only other known commercial source of yellow gem tourmaline. Whereas the Zambian material is elbaite, the Kenyan tourmaline is dravite-uvite (Mg-rich; see Simonet, 2000). Nevertheless, most of their physical properties overlap with two exceptions: (1) the Kenyan tourmalines have lower SG

Figure 20. These Vis-NIR absorption spectra were collected on the unheated (left) and heat-treated (right) tourmaline slices shown in figure 18 (2.59 mm thick). The Mn^{3+} absorption at 532 nm disappeared after heating to 550°C.

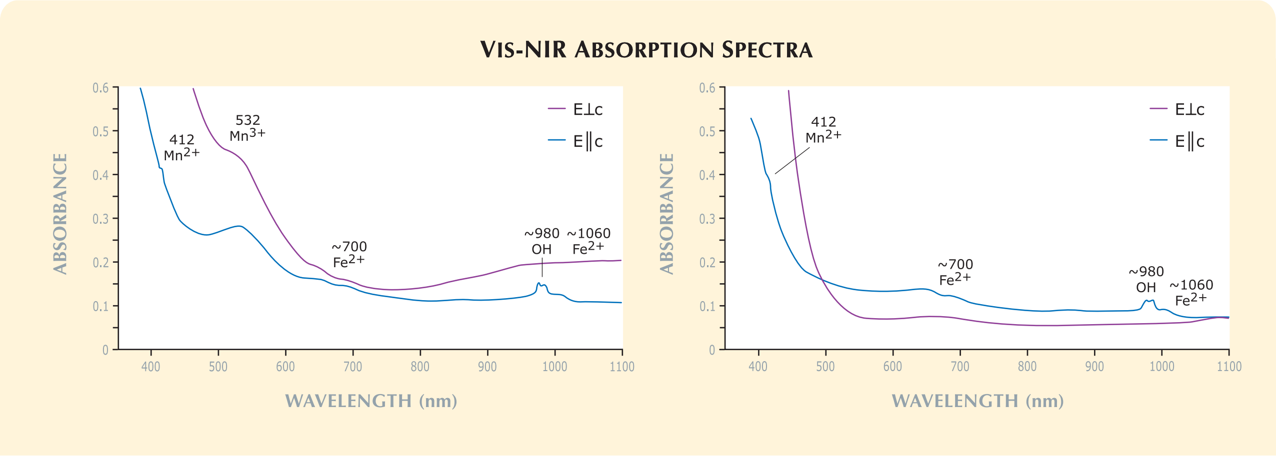

TABLE 2. Electron-microprobe analyses of tourmaline of various colors from the Canary mining area.[a]

Chemical composition	Grain mounts[b]									Faceted stones[b]	
	Greenish yellow	Yellow-brown	Pinkish brown	Bright yellow	Light brown	Light yellow	Yellow-green	Dk. brownish orange	Brownish orange[c]	Yellow	Yellowish green
Oxide (wt.%)											
SiO_2	36.26	36.22	36.33	36.34	36.32	36.56	36.58	36.58	36.59	36.64	36.54
TiO_2	0.31	0.33	0.24	0.41	0.44	0.17	0.14	0.15	0.13	0.43	0.10
B_2O_3 calc.	10.71	10.80	10.73	10.82	10.75	10.84	11.00	10.96	10.98	10.90	10.85
Al_2O_3	37.56	38.58	37.90	38.54	37.85	39.68	41.54	41.79	41.86	38.87	40.02
V_2O_3	0.15	nd	0.03	nd	0.02	nd	nd	nd	nd	nd	nd
FeO	nd	0.08	nd	nd	nd	nd	nd	nd	nd	nd	nd
MnO	7.39	7.16	6.61	6.34	6.33	4.41	2.68	1.52	1.31	6.21	4.00
MgO	nd	nd	nd	nd	nd	nd	nd	nd	0.05	nd	nd
CaO	0.03	0.06	0.08	0.40	0.46	0.03	0.02	nd	0.05	nd	nd
ZnO	nd	nd	nd	nd	nd	nd	nd	0.02	0.02	nd	nd
Li_2O calc.	1.32	1.29	1.44	1.48	1.54	1.59	1.75	1.82	1.88	1.51	1.60
Na_2O	2.48	2.47	2.65	2.43	2.50	2.44	2.54	2.34	2.47	2.40	2.36
K_2O	0.11	0.03	0.06	0.02	0.02	0.02	0.03	nd	0.02	0.02	0.01
H_2O calc.	3.20	3.19	3.24	3.28	3.46	3.26	3.25	3.21	3.27	3.22	3.19
F	1.05	1.13	0.98	0.97	0.53	1.01	1.16	1.21	1.10	1.15	1.17
Subtotal	100.56	101.33	100.30	101.05	100.22	100.01	100.68	99.58	99.72	101.36	99.85
-O=F	0.44	0.47	0.41	0.41	0.22	0.42	0.49	0.51	0.46	0.48	0.49
Total	100.12	100.86	99.89	100.64	100.00	99.58	100.20	99.07	99.26	100.88	99.36
Ions per 31 (O,OH,F)											
Si	5.884	5.825	5.885	5.834	5.869	5.860	5.779	5.802	5.790	5.840	5.856
T Al	0.116	0.175	0.115	0.166	0.131	0.140	0.221	0.198	0.210	0.160	0.144
Tet. sum	6.000	6.000	6.000	6.000	6.000	6.000	6.000	6.000	6.000	6.000	6.000
B calc.	2.999	2.999	2.999	2.999	2.999	2.999	2.999	2.999	2.999	3.000	3.000
Al Z	6.000	6.000	6.000	6.000	6.000	6.000	6.000	6.000	6.000	6.000	6.000
Al Y	1.067	1.138	1.121	1.127	1.078	1.355	1.514	1.613	1.598	1.142	1.414
V^{3+}	0.019	nd	0.003	nd	0.003	nd	nd	nd	nd	nd	nd
Ti	0.038	0.039	0.030	0.050	0.053	0.021	0.016	0.017	0.016	0.052	0.013
Fe^{2+}	nd	0.010	nd	nd	nd	nd	nd	nd	nd	nd	nd
Mn	1.015	0.975	0.907	0.863	0.866	0.598	0.359	0.204	0.176	0.838	0.543
Mg	nd	nd	nd	nd	nd	nd	nd	nd	0.012	nd	nd
Li calc.	0.859	0.835	0.938	0.958	0.999	1.026	1.110	1.163	1.195	0.967	1.030
Zn	nd	nd	nd	nd	nd	nd	nd	0.002	0.002	nd	nd
Y sum	2.999	2.999	2.999	2.999	2.999	2.999	2.999	2.999	2.999	3.000	3.000
Ca	0.006	0.011	0.014	0.069	0.079	0.004	0.003	nd	0.009	nd	nd
Na	0.782	0.769	0.832	0.757	0.785	0.759	0.778	0.718	0.757	0.743	0.734
K	0.024	0.005	0.013	0.003	0.004	0.004	0.006	nd	0.004	0.005	0.002
Vacancy	0.189	0.216	0.141	0.170	0.133	0.232	0.213	0.282	0.230	0.253	0.263
X sum	1.000	1.000	1.000	1.000	1.000	1.000	1.000	1.000	1.000	1.000	1.000
F	0.539	0.572	0.502	0.490	0.269	0.510	0.578	0.608	0.549	0.577	0.594
OH calc.	3.461	3.428	3.498	3.510	3.731	3.490	3.422	3.392	3.451	3.423	3.405
Mol.% tourmaline species											
Elbaite	80.0	77.3	84.3	76.0	78.7	76.3	78.3	71.8	76.0	74.6	73.6
Rossmanite	19.4	21.7	14.3	17.0	13.3	23.3	21.4	28.2	23.1	25.4	26.4
Liddicoatite	0.6	1.1	1.4	7.0	8.0	0.4	0.3	0.0	0.9	0.0	0.0

[a] *Cr, Cu, Bi, Ba, Pb, and Cl were analyzed for but not detected. Abbreviation: nd = not detected.*

[b] *Grain mounts were prepared by mounting pieces taken from rough samples in epoxy and polishing them smooth; representative analyses are shown for the main colors analyzed, and arranged by decreasing Mn content. For the faceted stones, the average of five analyses across the table of each sample is shown for the stones with the highest and lowest Mn contents.*

[c] *This sample was also used for heat treatment (it became yellow; see figure 18) and spectroscopy.*

values; and (2) it is not uncommon for the Kenyan stones to fluoresce yellow to short-wave UV radiation, while the Zambian tourmaline is inert.

Raman spectra of a yellowish green Canary tourmaline sample are available at http://rruff.info (sample R070077). A Raman peak located at ~850

Figure 21. The vivid yellow color of Canary tourmaline is quite distinctive for gem elbaite. The relatively large examples shown here weigh 25.00 ct (pear), 18.00 ct (oval), and approximately 6 ct each (smaller pear shapes). Courtesy of Joeb Enterprises; photo by Robert Weldon.

cm^{-1} in the spectra is stronger than in any other tourmaline analyzed for the RRUFF database, with the exception of the dark green portion of a color-zoned Mn-poor sample from Brazil (R060566; R. Downs, pers. comm., 2007). The origin of this strong Raman peak is unknown.

Chemical Composition. In addition to the Lundazi District of Zambia, significant occurrences of yellow Mn-rich elbaite are known from Tsilaisina in central Madagascar (Duparc et al., 1910), Elba Island in Italy (Bosi et al., 2005), Austria (Ertl et al., 2003, 2004), Nepal (Rossman and Mattson, 1986; Burns et al., 1994), the Malkhan District in Russia (Mashkovtsev and Zagorsky, 1997), and the Pamir Mountains in Tajikistan (Mashkovtsev and Zagorsky, 1997). Recently, substantial amounts of this tourmaline have come from the Muva area in Mozambique (unpublished data of BML and WBS).

The highest Mn content found in the samples analyzed for this study was 7.59 wt.% MnO. This is considerably less than the 9.18 wt.% MnO measured by Shigley et al. (1986), which approaches "tsilaisite" composition (i.e., 10.7 wt.% MnO needed to attain a 50:50 ratio of tsilaisite:elbaite). Schmetzer and Bank (1984b) reported 6.3–6.9 wt.% MnO in a yellow Zambian tourmaline, and Rossman and Mattson (1986) measured 6.18–6.85 wt.% oxide in their yellow to yellow-green samples. These values are similar to the higher Mn contents measured in this study, but our values ranged considerably lower (1.14 wt.%) among the greenish yellow to yellow to brownish yellow samples we analyzed (see *G&G* Data Depository). The maximum Mn contents measured in our samples are only about two-thirds the amount needed to attain a "tsilaisite" composition (figure 17).

Kunitz (1929) documented a systematic decrease in RI values with lower Mn content in elbaite. The limited range of RI values obtained for the polished stones in this study (table 1) is consistent with the rather narrow range of Mn contents (~4–6.5 wt.% MnO; see *G&G* Data Depository) that was measured in eight of these stones by electron microprobe analysis.

Cause of Color. The yellow-green coloration is due to a Mn^{2+} plus Mn^{2+}-Ti^{4+} intervalence charge transfer interaction that is responsible for absorbing the violet-to-blue portion of the spectrum (Rossman and Mattson, 1986). Variations from greenish yellow to yellow to brown are due to Fe^{2+}-Ti^{4+} IVCT; in contrast, the green color of typical elbaites from granitic pegmatites is associated with much higher Fe and lower Ti contents (Rossman and Mattson, 1986).

The unheated brownish orange tourmaline (again, see figure 18) initially owed its color to a superposition of a Mn^{3+} absorption centered in the 530 nm region of the tourmaline spectra. After heating for two hours at 550°C, the sample lost the 530 nm absorption band and turned yellow. It has long been recognized that Mn^{3+} can be thermally reduced to Mn^{2+} by heating pink tourmaline at temperatures between 500°C and 600°C (Reinitz and Rossman, 1988). However, heating to higher temperatures causes the Mn^{2+} to be re-oxidized to Mn^{3+} and create pink color, as shown in box A.

The Mn^{2+} and Mn^{2+}-Ti^{4+} IVCT features in the spectra of the heated brownish orange tourmaline were not significantly altered. It follows, then, that yellow-green Canary tourmaline does not change color on heating to 500–600°C because it does not contain the Mn^{3+} component.

Formation of Canary Tourmaline. Gem tourmaline typically consists of pink, green, or blue elbaite that is mined from the lepidolite-bearing inner zones of complex LCT (lithium, cesium, tantalum) pegmatites. In contrast, Mn-rich (and Ti-bearing) yellow elbaite from the Canary mining area appears to have formed in a pegmatite with a simpler mineralogy. The enrichment of Mn in granitic pegmatites is usually associated with significant amounts of Li (Černý et al., 1985), leading to its incorporation into

Li-micas or Li-phosphates. Spessartine crystallization is an even more important mechanism for depleting Mn from the pegmatite system, and the Mn content of tourmaline has been shown to be influenced by the abundance of garnet in the pegmatite (Novák et al., 2000). Although minor amounts of spessartine were observed by one of us (BA) in a tailings pile at the Canary mine, we infer that it was not a common mineral in the pegmatite. We suggest that the rarity of Mn-rich yellow elbaite in nature is due to the need for an unusual combination of high B and Mn with low Li in pegmatite-forming magma.

The formation of Canary tourmaline required that Mn (and some Ti) was conserved until the final stage of pegmatite crystallization (in gem pockets). However, the bright yellow coloration of this tourmaline (natural or after heat treatment) will only develop in the absence of significant Fe. The most likely mechanism for conserving Mn while depleting Fe is early crystallization of abundant schorl, since Fe is much more compatible in schorl than Mn (Wolf and London, 1997; London et al., 2001). Although little primary schorl was seen in the remaining portions of the pegmatite footwall during our visit, we saw abundant black tourmaline in an earlier photo of the pegmatite.

The enriched B content of the original pegmatite magma promoted schorl crystallization, rather than the formation of micas or spessartine (which would deplete Mn). The formation of schorl also consumed some Ti, but schorl is much less efficient than biotite at scavenging Ti from the pegmatite melt (Icenhower and London, 1995). Therefore, since biotite was apparently absent from the Canary pegmatite, there was still enough Ti available during the crystallization of the gem pockets to develop the yellow color in Canary tourmaline via Mn^{2+}-Ti^{4+} intervalence charge transfer.

Following pegmatite crystallization, the influx of an unusual B-, Fe-, K- and Na-rich fluid (apparently from an external source) resulted in local tourmaline ± K-feldspar + albite veining and quartz dissolution; the same event also brecciated some of the yellow elbaite with black tourmaline ± K-feldspar + albite assemblages.

CONCLUSION

This study presents additional information on Mn-rich yellow gem tourmaline from the Lundazi District of eastern Zambia. The principal source of this elbaite is the Canary mining area, where it has been mined from eluvial/alluvial and primary (pegmatite) deposits since the early 1980s. The gemological properties are typical of elbaite, but the chemical composition is notable for high Mn and low Fe combined with relatively enriched Ti for gem tourmaline. This composition probably resulted from the evolution of a B-rich, Li-poor granitic pegmatite in which early crystallization of abundant schorl removed the Fe while conserving Mn until the late-stage formation of gem tourmaline–bearing pockets.

Most of the tourmaline is heat treated to 500–550°C to reduce the brown/orange component. Although some relatively large stones have been faceted (e.g., figure 21), most are <1 ct. Considering the amount of Canary tourmaline that has been sold into marketplace, it is still relatively uncommon to encounter it in jewelry (figure 22). Although the potential reserves of this tourmaline are unknown, abundant melee could be cut from the current stockpiles of rough, and additional mining is expected to increase the availability of larger material.

Figure 22. Canary tourmaline is set with diamonds in this ring (2.28 ct center stone) and pair of earrings. Ring courtesy of Tommy Wu, and earrings are from Henry Jewelry Inc., Los Angeles; photo by Robert Weldon.

ABOUT THE AUTHORS

Mr. Laurs (blaurs@gia.edu) is editor of Gems & Gemology *at GIA in Carlsbad. Dr. Simmons is professor of mineralogy and university research professor, and Mr. Falster is senior research technologist, at the University of New Orleans, Louisiana. Dr. Rossman is professor of mineralogy at the California Institute of Technology, Pasadena. Mr. Fritz is staff gemologist, and Mr. Koivula is chief gemologist, at the GIA Laboratory in Carlsbad. Mr. Anckar is gemologist/geologist with Mayfair Mining & Minerals Inc., Lindfield, West Sussex, England.*

ACKNOWLEDGMENTS

The authors are grateful to Tommy Wu (Shire Trading Ltd., Hong Kong) for providing logistical support in the field and access to the mining property, as well as supplying information and loaning/donating samples for research. We also thank Rita and Arun Mittal (Southstream Enterprises Ltd., Lusaka, Zambia) for providing information and samples during the authors' visit to Zambia. Useful insights on the geology were provided by mine geologist Naveen Torgalmoth, who tragically died of malaria in 2006. Robert Downs (University of Arizona, Tucson) provided assistance with interpreting the Raman spectrum of Canary tourmaline.

REFERENCES

Boehm E. (2001) Gem News International: Canary tourmaline from Malawi. *Gems & Gemology*, Vol. 27, No. 2, pp. 151–152 (see erratum in Vol. 40, No. 1, p. 86).

Bosi F., Agrosì G., Lucchesi S., Melchiorre G., Scandale E. (2005) Mn-tourmaline from island of Elba (Italy): Crystal chemistry. *American Mineralogist*, Vol. 90, pp. 1661–1668.

Burke E.A.J. (2006) A mass discreditation of GQN minerals. *Canadian Mineralogist*, Vol. 44, pp. 1557–1560.

Burns P.C., MacDonald D.J., Hawthorne F.C. (1994) The crystal chemistry of manganese-bearing elbaite. *Canadian Mineralogist*, Vol. 32, pp. 31–41.

Capturing the Canary yellow tourmaline (2003) *Idex Magazine*, Vol. 18, No. 158, pp. 89–91.

Černý P., Meintzer R.E., Anderson A.J. (1985) Extreme fractionation in rare-element granitic pegmatites: Selected examples of data and mechanisms. *Canadian Mineralogist*, Vol. 23., pp. 381–421.

Dunn P.J., Fleischer M., Langley R., Shigley J.E., Zilczer J.A. (1985) New mineral names. *American Mineralogist*, Vol. 70, pp. 871–881.

Duparc L., Wunder M., Sabot R. (1910) Les minéraux des pegmatites des environs d'Antsirabé a Madagascar. *Mémoires de la Société de physique et d'Histoire Naturalle de Genève*, Vol. 36, No. 3, pp. 283–410.

Ertl A., Hughes J.M., Prowatke S., Rossman G.R., London D., Fritz E.A. (2003) Mn-rich tourmaline from Austria: Structure, chemistry, optical spectra, and relations to synthetic solid solutions. *American Mineralogist*, Vol. 88, pp. 1369–1376.

Ertl A., Schuster R., Prowatke S., Brandstätter F., Ludwig T., Bernhardt H.-J., Koller F., Hughes J.M. (2004) Mn-rich tourmaline and fluorapatite in a Variscan pegmatite from Eibenstein an der Thaya, Bohemian massif, Lower Austria. *European Journal of Mineralogy*, Vol. 16, pp. 551–560.

Federman D. (2002) Gem Profile—Canary tourmaline: Miracle from Malawi. *Modern Jeweler*, Vol. 101, No. 1, pp. 45–46.

Genis R. (2001) Canary yellow tourmaline makes grand entrance. *Rapaport Diamond Report*, Vol. 24, No. 35, pp. 123, 125.

Hänni H.A., Frank E., Bosshart G. (1981) Golden yellow tourmaline of gem quality from Kenya. *Journal of Gemmology*, Vol. 17, No. 7, pp. 437–442.

Icenhower, J.P., London, D. (1995) An experimental study of element partitioning between biotite, muscovite and coexisting peraluminous granitic melt at 200 MPa (H_2O). *American Mineralogist*, Vol. 80, pp. 1229–1251.

Johns C.C., Liyungu K., Mabuku S., Mwale G., Sakungo F., Tembo F., Vallance G. (1989) The stratigraphic and structural framework of eastern Zambia. *Journal of Applied Earth Sciences*, Vol. 9, No. 1, pp. 123–136.

Johnson M.L., Koivula J.I., Eds. (1996) Gem News: Golden tourmaline from Kenya. *Gems & Gemology*, Vol. 32, No. 2, pp. 135–136.

Johnson M.L., Wentzell C.W., Elen S. (1997) Multicolored bismuth-bearing tourmaline from Lundazi, Zambia. *Gems & Gemology*, Vol. 33, No. 3, pp. 204–211.

Kane R.E. (1986) Gem Trade Lab Notes: Tourmaline, unusual yellowish green. *Gems & Gemology*, Vol. 22, No. 3, pp. 175–176.

Kunitz W. (1929) Betrage zur Kenntnis der magmatischen Assoziationen I. Die Mischungsreihen in der Turmalingruppe und die genetischen Beziehungen zwischen Turmalinen und Glimmern. *Chemie der Erde*, Vol. 4, pp. 208–251.

Laurs B.M. (2004) Gem News International: Update on several gem localities in Zambia and Malawi. *Gems & Gemology*, Vol. 40, No. 4, pp. 347–350.

London D., Evensen J.M., Fritz E., Icenhower J.P., Morgan G.B., IV, Wolf M.B. (2001) Enrichment and accommodation of manganese in granite-pegmatite systems. In *Eleventh Annual V. M. Goldschmidt Conference*, Abstract #3369, LPI Contribution No. 1088, Lunar and Planetary Institute, Houston (CD-ROM).

Mashkovtsev R.I., Zagorsky V.E. (1997) Spectroscopic study of Mn-bearing elbaites. *Tourmaline 1997*, June 20–25, Moravian Museum, Brno, Czech Republic, p. 54.

Mattson S.M., Rossman G.R. (1987) Fe^{2+}-Fe^{3+} interactions in tourmaline. *Physics and Chemistry of Minerals*, Vol. 14, pp. 163–171.

Milisenda C.C., Malango V., Taupitz K.C. (2000) Edelsteine aus Sambia—Teil 2: Turmalin und aquamarin. *Gemmologie: Zeitschrift der Deutschen Gemmologischen Gesellschaft*, Vol. 49, pp. 31–48.

Njamu F.M. (2003) Survey of productive mines in Nyimba, Petauke, Chadiza and Lundazi Districts, Eastern Province, Zambia. Unpublished report prepared on behalf of Lundazi Gemstone Association in cooperation with Mining Sector Diversification Programme and Zambia Trade Investment Enhancement, Lusaka, 129 pp.

Novák M., Selway J.B., Černý P., Chapman R.C., Masau M. (2000) Correlation between Mn content in tourmaline and garnet abundance in two elbaite-subtype pegmatites: Dolní Rožínka and Pikárec, Czech Republic. *Geological Association of Canada—Mineralogical Association of Canada, Joint Annual Meeting*, abstract #584.

Nuber B., Schmetzer K. (1984) Structural refinement of tsilaisite (manganese tourmaline). *Neues Jahrbuch für Mineralogie, Monatshefte*, Vol. 7, pp. 301–304.

O'Connor E.A. (1998) *Geology of the Lumezi River and Lundazi areas—Explanation of Degree Sheets 1232 NE Quarter and Parts of 1233 NW and NE Quarters*. Geological Survey Department Report No. 71, Lusaka, 29 pp., 2 maps.

Patney R.K., Tether J. (1988) The gem bearing pegmatites of eastern Zambia. *Zambian Journal of Applied Earth Sciences*, Vol. 2, No. 2, pp. 41–53.

Pieczka A., Kraczka J. (2004) Oxidized tourmalines—A combined chemical, XRD and Mössbauer study. *European Journal of Mineralogy*, Vol. 16, pp. 309–321.

Reinitz I.L., Rossman G.R. (1988) Role of natural radiation in tourmaline coloration. *American Mineralogist*, Vol. 73, pp. 822–825.

Rossman G.R., Mattson S.M. (1986) Yellow, Mn-rich elbaite with Mn-Ti intervalence charge transfer. *American Mineralogist*, Vol. 71, pp. 599–602.

Schmetzer K., Bank H. (1983) Intensiv gelb gefärbter Tsilaisite (Manganturmalin) von Edelsteinqualität aus Sambia. *Zeitschrift der Deutschen Gemmologischen Gesellschaft*, Vol. 32, No. 4, pp. 159–163.

Schmetzer K., Bank H. (1984a) Crystal chemistry of tsilaisite (manganese tourmaline) from Zambia. *Neues Jahrbuch für Mineralogie, Monatshefte*, Vol. 2, pp. 61–69.

Schmetzer K., Bank H. (1984b) Intensive yellow tsilaisite (manganese tourmaline) of gem quality from Zambia. *Journal of Gemmology*, Vol. 19, No. 3, pp. 218–223.

Shigley J.E., Kane R.E., Manson D.V. (1986) A notable Mn-rich gem elbaite tourmaline and its relationship to "tsilaisite." *American Mineralogist*, Vol. 71, pp. 1214–1216.

Simonet C. (2000) Geology of the Yellow mine (Taita-Taveta District, Kenya) and other yellow tourmaline deposits in East Africa. *Journal of Gemmology*, Vol. 27, No. 1, pp. 11–29.

Snelling N.J., Johnson R.L., Drysdall A.R. (1972) The geochronology of Zambia. *Records of the Geological Survey of Zambia*, Vol. 12, pp. 19–30.

Substantial increase in sales of Canary tourmaline: Japanese trader (2005) *Jewellery News Asia*, No. 245, pp. 66, 68.

Supplier to vertically integrate mining, polishing and wholesaling of Zambian yellow tourmaline (2004) *Jewellery News Asia*, No. 236, pp. 128, 138, 140.

Thomas A.E. (1982) Zambian tourmaline. *Journal of Gemmology*, Vol. 18, pp. 4–6.

Wolf M.B., London D. (1997) Boron in granitic magmas: Stability of tourmaline in equilibrium with biotite and cordierite. *Contributions to Mineralogy and Petrology*, Vol. 130, pp. 12–30.

Wong M. (2001) IJT 2001 reports slower traffic but similar sales. *Jewellery News Asia*, No. 199, pp. 208–210.

Zgambo N. (1995) The Lundazi aquamarine pegmatites of eastern Zambia. *International Conference on Industrial Minerals Proceedings*, Lusaka, Zambia, publ. by Council for Geosciences, Pretoria, South Africa, pp. 226–239.